JMEPEG (2015) 24:3433–3443
DOI: 10.1007/s11665-015-1630-y

1059-9495/$19.00

Electrochemical and Morphological Study of Steel in 1 M HCl in the Presence of Task Specific Liquid

F.S. Tabatabaei, A.A. Sarabi, E. Kowsari, and H. Eivaz Mohammadloo

(Submitted September 25, 2014; in revised form July 3, 2015; published online August 5, 2015)

In the present study, corrosion inhibition influence of novel cationic surfactant (CS) with imidazole structure (1-methyl-3-octadecane imidazolium hydrogen sulfate) on low carbon steel in 1 M HCl was investigated by implementing weight loss, potentiodynamic polarization, and electrochemical impedance spectroscopy (EIS) techniques. Increasing the amount of surfactant adequately leads to an increment of the inhibition efficiency of novel CS. According to the obtained results from EIS measurements, inhibition efficiency was about 34% in the presence of 1 ppm surfactant, increasing to about 96.8% at the 25 ppm (near critical micelle concentration) surfactant concentration. Also the effects of temperature and the synergistic effect between surfactant and $NaHSO_4$ salt were studied. The inhibition efficiency increased with the increase of $NaHSO_4$ concentration and reached the maximum value near 0.1 M and experienced a plummet in the temperature range of 30-50 °C. Potentiodynamic polarization measurements revealed that the surfactant acts as mixed-type inhibitors. Results obtained from weight loss, polarization, and impedance measurements are in proper agreement and confirmed the fact that this surfactant is an excellent inhibitor for low carbon steel in 1 M HCl environment. The surface morphology of inhibited and uninhibited metal samples was investigated by atomic force microscope (AFM) and field emission scanning electron microscope (FE-SEM).

Keywords atomic force microscopy (AFM), corrosion, electrochemical impedance spectroscopy, electrochemistry, scanning electron microscopy, metals

1. Introduction

Hydrochloric acid solutions are commonly used in petroleum fields and several industries with the purpose of cleaning and de-scaling of iron and steel alloys (Ref 1). Usage of corrosion inhibitors, surfactants for instance, leads to reduction of corrosion rate of metallic materials in acidic media. For the sake of iron and steel alloys protective behavior, recently, surface-active agents (surfactants) have been widely used as corrosion inhibitors in this regard. The adsorption of the surfactants on metal surface can markedly change the properties of the metal in terms of corrosion resistance; therefore the investigation of the relations between the adsorption and corrosion inhibition should be taken under the consideration (Ref 1, 2).

Heterocyclic organic compounds containing nitrogen, sulfur, or oxygen atoms are often used to protect metals from corrosion. Among them, it has been proven that azoles are effective copper corrosion inhibitors (Ref 2, 3). Surfactants are amphiphilic molecules, which exhibit a double affinity for polar and non-polar substances. In its simplest configuration, a surfactant molecule has two types of functional groups, a hydrophilic or polar group (water-soluble), and a lipophilic or non-polar group (oil-soluble), which is generally a long chain hydrocarbon (Ref 4). Inhibition of surfactants is described by adsorption on the metal surface (Ref 5). Definite physicochemical characteristics of the surfactant molecule, such as, functional groups, aromaticity, orbital character of the donating electrons, steric effect, electron density on the donor atoms, and the electronic structure of the molecule, have substantial effect on the adsorption ability of the surfactant (Ref 6-8). In addition, the application of cationic surfactants as corrosion inhibitors of metal has been widely studied (Ref 9-11).

Mostly studies focused on hydrochloric acidic medium, since better inhibition performance of surfactants in HCl was gained in comparison with sulphuric acid solutions (Ref 2). The use of hydrochloric acid in pickling of metals, acidization of oil wells, and cleaning of scales is more economical, efficient, and trouble-free, than other mineral acids (Ref 12). In corrosion inhibition with surfactant inhibitors, the critical micelle concentration (CMC) is non-neglectable and the most important parameter to predict surfactant performance. Due to the fact that metallic surface can be blocked by added surfactants, corrosion reaction decreases when the concentration of absorbed surfactant is high enough (Ref 2, 4, 5).

The aim of this article is to use novel cationic surfactant with imidazole structure as a green inhibitor to study the compatibility and effectiveness of this structure on low carbon steel corrosion properties in aerated 1 M HCl solution. The effect of inhibitor concentration on the performance and extent of adsorption of CS were studied using weight loss and electrochemical AC and DC techniques. The steel surface was also examined by atomic force microscope (AFM) and field emission scanning electron microscope (FE-SEM).

F.S. Tabatabaei and **E. Kowsari**, Department of Chemistry, Amirkabir University of Technology (Tehran Polytechnic), Tehran, Iran; and **A.A. Sarabi** and **H. Eivaz Mohammadloo**, Faculty of Polymer Engineering & Color Technology, Amirkabir University of Technology (Tehran Polytechnic), Tehran, Iran. Contact e-mail: sarabi@aut.ac.ir.

2. Experimental Methods and Materials

2.1 Materials

2.1.1 Substrate. Tests were performed on low carbon steel of the following composition (wt.%): 0.06 C, 0.06 Si, 0.7 Mn, 0.002 V, 0.005 P, 0.001 S, 0.012 Ni, 0.015 Cr, 0.004 Mo, 0.02 Cu, and 99.12 Fe.

2.1.2 Surfactant. The surfactant (1-methyl-3-octadecane imidazolium hydrogen sulfate) was synthesized according to previous work (Ref 13) and its chemical structure is shown in Fig. 1. It is evident that this CS is an *N*-heterocyclic compound containing two nitrogen atoms.

2.1.3 Solutions. The aggressive solution of 1 M HCl was prepared by dilution of analytical grade 37 wt.% HCl from Merck Co. with distilled water. The concentration range of inhibitor used was 1-200 mg/L. All solutions were prepared using distilled water. $NaHSO_4$ salt was obtained from Merck.

2.2 Surface Tension Measurements

The surface tension measurements of the synthesized cationic surfactants were conducted utilizing Du Nouy ring tensiometer (Kruss 8451) for various concentrations of the inhibitor at 25 ± 2 °C. Doubly distilled water with a surface tension of ca. 72 mN/m was used to prepare all solutions.

2.3 Weight Loss Measurements

Rectangular specimens of low carbon steel (30 mm × 20 mm × 1.5 mm) were mechanically abraded with 600, 800, 1000, and 1200 grades of emery paper. They were degreased with acetone and rinsed with distilled water two times. Then they were immersed in 0.5 M HCl solution for 10 s (acid pickling), rinsed with distilled water two times and finally dried. After weighing accurately, the specimens were immersed in 250 cc beaker, which contained 150 cc of 1 M HCl, once without any surfactants and on other occasion with different concentrations of surfactant. All the aggressive acid solutions were open to air. After 1 h, the specimens were taken out, washed with distilled water, dried, and weighted using an analytic balance (precision: 0.1 mg). The corrosion rate and inhibition efficiency (IE_{wl} %) are calculated as follows (Ref 14-16):

$$IE_{wl}\% = 1 - r/r' \quad \text{(Eq 1)}$$

$$r = (m_1 - m_2)/St \quad \text{(Eq 2)}$$

where r and r' (g/m^2/h) are the corrosion rate of steel with and without the addition of surfactant in HCl solution, respectively. The m_1 (g) represents the weight of steel before immersion and m_2 (g) is the weight of steel after immersion in solution. S (m^2) and t (h) are the surface area of the steel sheet and the corrosion time, respectively.

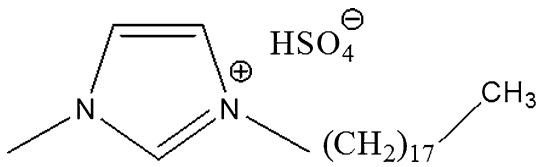

Fig. 1 The chemical structure of surfactant

2.4 EIS and Potentiodynamic Polarization Tests

Electrochemical impedance spectroscopy and potentiodynamic polarization measurements were done in a three-electrode system (a platinum counter-electrode and Ag/AgCl electrode as reference). The low carbon steel electrode was sealed with epoxy resin and only the cross-section of 1 cm^2 area was open to the electrolyte. The experiments were carried out at constant temperature (25 ± 1 °C). Prior to implementing the test, it is mandatory to reach a steady state of potential; therefore, the electrode was immersed in the test solution for 1 hour at open circuit potential to attain steady state condition. All polarization curves were derived by AUTOLAB PGSTAT 302 N. The potential increased with the rate of 1 mV/s and started from potential of −100 mV to +100 mV versus corrosion potential (E_{corr}). The inhibition efficiency is calculated employing the following equation (Ref 17, 18):

$$IE_{pol}\% = (i_{corr} - i_{corr(inh)})/i_{corr} \quad \text{(Eq 3)}$$

where i_{corr} and $i_{corr(inh)}$ are the corrosion current densities. The former is assigned to corrosion current density in the absence of the inhibitor and the latter stands for corrosion current density in the presence of the inhibitor. The corrosion current density (i_{corr}) values were obtained by extrapolation of cathodic and anodic regions. EIS experiments were executed in a frequency range of 100 kHz to 0.01 Hz with 10 mV perturbations (peak to peak) by using AUTOLAB PGSTAT 302 N. The acquired data were curve fitted and analyzed using Nova 1.8 software. At least three samples were repeated in each experiment to get reproducible results.

2.5 Surface Examination

The low carbon steel specimens were also treated with the same method as in section 2.3. After immersion of samples in 1 M HCl at 25 °C for 1 h, all the samples (including those without surfactants) were cleaned with deionized water, dried with a cold air blaster and then studied by Denmark instrument model DS 95-50-E scanner AFM. Also an investigation into their morphological behavior was conducted through Field Emission Scanning Electron Microscope (FE-SEM; Hitachi, Model S4161). Prior to SEM examination, the samples were sputter-coated with a layer of gold in order to enhance picture sharpness.

3. Results and Discussion

3.1 Effect of CS Concentration

3.1.1 Surface Tension. Diffusion of surfactant from a bulk phase to an interface, such as gas/liquid, liquid/liquid, and liquid/solid interface, comes with the reduction of the surface or interfacial tension (Ref 19). The results for surface tension were plotted versus the surfactant concentration and the critical micelle concentration which was estimated from the break-point in the resulting curve (Ref 20, 21). The CMC is influenced by a number of distinct circumstances that are dependent on the nature of surfactant, the nature of the created dispersion in the aqueous environment, and the method used for determination. A linear trend for reduction in surface tension was perceived with increase in concentrations for cationic surfactants up to the CMC, beyond which no significant change

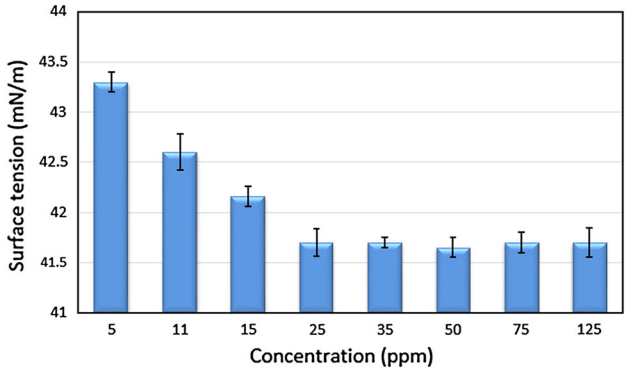

Fig. 2 Surface tension measurements of surfactant at 25 °C

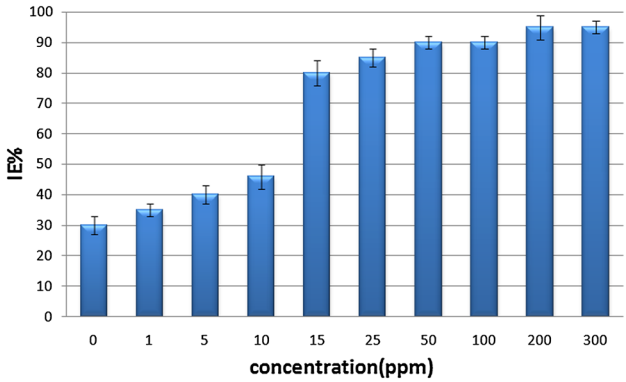

Fig. 3 Variation of inhibition efficiency in 1 M HCl in the presence of different concentrations of surfactant (1-200 ppm)

was observed. In this paper, the CMC is determined by measurement of the surface tension (γ). Determination of the CMC is of great importance because at this concentration, most of the physical and chemical properties of the surfactant's solution undergo an abrupt change (Ref 12, 22). Figure 2 illustrates the variations of surface tension with the surfactant concentration. The results demonstrated that the surface tension virtually remains constant at concentrations greater than the CMC. While for smaller concentrations, as the concentration decreases, the surface tension rises proportionally (Ref 19, 22, 23). According to Fig. 2, the CMC of novel cationic surfactant is roughly 25 ppm.

3.1.2 Weight Loss Measurements. Different experimental techniques can be used to evaluate corrosion rate and inhibition efficiency of low carbon steel. Weight loss method is one of the simplest methods (Ref 15, 20, 24). Corrosion rates of low carbon steel in the absence and presence of the surfactant at various concentrations in the range of 0-200 ppm in 1 M HCl were gained. Acquired data reveal that the corrosion rate diminishes from 0.33 g/m^2/h in blank solution to 0.05 g/m^2/h in presence of 25 ppm and 0.016 g/m^2/h as surfactant concentration increases up to 200 ppm.

By utilizing Eq 1, the inhibition efficiencies of the surfactant on steel corrosion at various concentrations were calculated. Equation 1 is shown in Fig. 3 and Table 1 in details. Inhibition efficiency soared from 46 to 90% as the surfactant concentration increases from 10 to 50 ppm and a moderate (Ref 7) adsorption takes place. As it can been seen in Fig. 3, the inhibition efficiency rose and then leveled off with increase in inhibitor concentration.

Table 1 Calculated corrosion rates (R_{corr}) and inhibition efficiencies (IE_{wl}) in 1 M HCl solutions after 1 h of immersion at 25 °C, calculated from the weight loss test

Concentration (ppm)	Δm (mg)	R_{corr} (g/m^2/h)	IE%
Blank	2	0.33	…
1	1.3	0.216	35
5	1.1	0.2	40
10	1.1	0.183	46
15	0.4	0.066	80
25	0.3	0.05	85
50	0.2	0.033	90
100	0.2	0.033	90
200	0.1	0.016	95

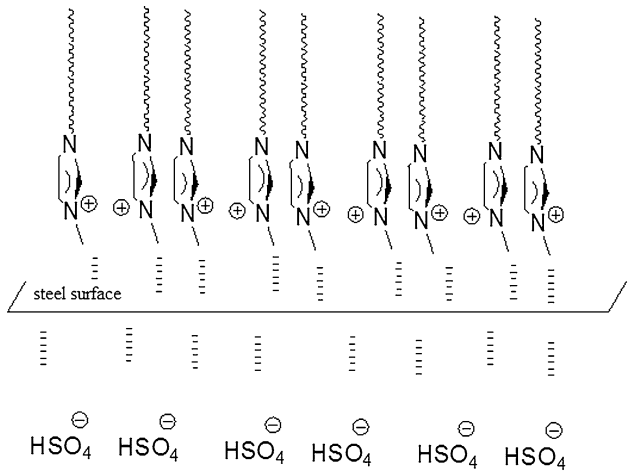

Fig. 4 Schematic of surfactant molecules adsorption on low carbon steel surface in acidic medium

Surfactant inhibitory behavior is not simply an indication of electrostatic adsorption (Ref 23-25). It might be attributed to the way that HSO_4^- anions of surfactant are influential and chemisorption of 1-methyl-3-octadecane imidazolium ions occurs on steel. Moreover, other factors such as CMC and structure of surfactant make an impact on inhibition efficiency (Ref 15, 26).

The adsorption is favored by electrostatic and chemisorption interactions between the ammonium groups (N^+) and cathodes sites and HSO_4^- on the metallic surface.

The model of an electrical double layer with specifically adsorbed CS on a metallic surface is shown in Fig. 4. When there is not enough CS to cover the metal surface and the adsorption rate is low, metal dissolution occurs on the low carbon steel surface free of CS. With high amount of surfactant, an intact CS over layer is deposited on low carbon steel that leads to reduction of chemical attacks on the metal surface (Ref 27-29).

3.1.3 Electrochemical Measurements. Corrosion behavior of steel and the effect of surfactant concentration on low carbon steel were studied by using EIS measurements in 1 M HCl in the absence and presence of CS at 1 h immersion at 25 °C. Nyquist plots are shown in Fig. 5. It is clear from the plots that the impedance response of low carbon steel in 1 M HCl solution was significantly changed after the addition of the

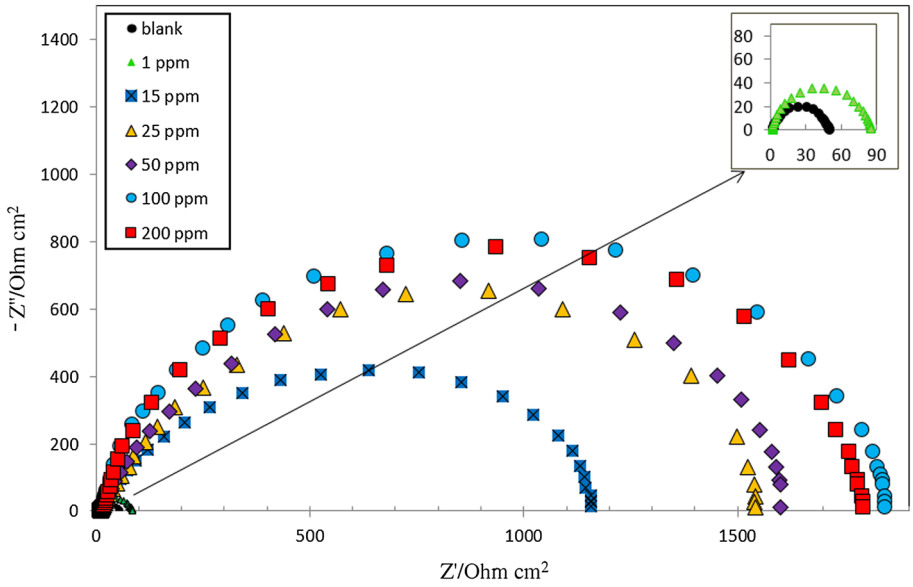

Fig. 5 Nyquist plots for carbon steel in 1 M HCl in the absence and presence of different concentrations of CS at 25 °C

Table 2 Data obtained from electrochemical impedance measurements of low carbon steel in 1 M HCl solution in absence and presence of various concentrations of the CS

CS concentration (ppm)	R_{ct} (Ω cm^2)	n	Y_0	C_{dl} (μF/cm^2)	IE%
0	52.2	0.9	154	86.2	…
1	80.1	0.93	115	73.3	34
25	1730	0.79	85.4	19.1	96.9
50	1900	0.81	75.7	20.6	97.2
100	1950	0.77	86.4	25.6	97.3
200	1910	0.76	56.9	25.5	97.2

surfactant molecules. The Nyquist curve contains a single capacitive semicircle for low carbon steel electrode in 1 M HCl and in the presence of CS molecule this states that during anodic dissolution of low carbon steel, only a single charge transfer process took place; the corrosion process of low carbon steel was controlled by charge transfer on the surface of the metal.

The electrical equivalent circuit for electrode-electrolyte interface is shown inset of Fig. 5. In this figure, R_s, R_{ct}, and CPE represent solution resistance, charge transfer resistance at metal-electrolyte interface, and non-ideal double-layer capacitance, respectively. Constant phase element (CPE) was used instead of capacitance in this work. The utilization of CPE instead of double-layer set of capacitance (C_{dl}) could be linked to the more accurate fit in the case of deviation from an ideal capacitor.

All the parameters including solution resistance R_s, charge transfer resistance R_{ct}, double-layer capacitance C_{dl}, and percentage inhibition efficiency (IE_{EIS} %) are calculated and listed in Table 2. The capacitance values were calculated according to the following equation:

$$C_{dl} = \left(Y_0 R_{ct}^{1-n}\right)^{1/n} \quad \text{(Eq 4)}$$

where Y_0 is the magnitude of admittance of the CPE (in $S^n/\Omega/cm^2$) and n is the CPE exponent, as $n = \alpha/(\pi/2)$ (α is the constant phase angle of the CPE). The n value indicates a phase shift and can characterize different surface phenomena such as surface heterogeneity (in-homogeneity) resulting from surface roughness, dissolution of the metal, impurities, distribution of the active sites, inhibitor adsorption or porous layer formation (Ref 30, 31). The IE_{EIS} was calculated from the values of R_{ct} using Eq 5 (Ref 24).

Table 3 potentiodynamic polarization parameters for low carbon steel in 1 M HCl containing different concentrations of CS by the Tafel extrapolation method

Inhibitor system (ppm)	i_{corr} (μA/cm^2)	E_{corr} (V vs. Ag/AgCl)	IE%
0	200	−0.484	…
1	82	−0.475	59
25	31	−0.466	84.5
50	28.2	−0.43	85.9
100	22	−0.446	89
200	19	−0.454	90.5

$$IE_{EIS}\% = (R_{ct(inh)} - R_{ct})/R_{ct(inh)} \quad \text{(Eq 5)}$$

where $R_{ct(inh)}$ and R_{ct} are the charge transfer resistance values with and without inhibitors, respectively. Increase in charge transfer resistance R_t and reduction of the double-layer capacitance C_{dl} at the same time with increasing the inhibitor concentration reveals that this surfactant positively influences the corrosion rate of low carbon steel in 1 M HCl solution by adsorption at the metal-solution interface mechanism (Ref 20, 32). In the presence of surfactants, the transfer resistance in acidic solution rises, as well as a decrease in local dielectric constant and/or an increase in the thickness of the electrical double layer.

The value of R_{ct} increases from 52.2 (Ω cm^2) in the absence of any surfactant to 1730 (Ω cm^2) in presence of 25 ppm of the surfactant. This behavior reveals the adsorption of inhibitors on steel, and indicates an increase in the corrosion inhibition

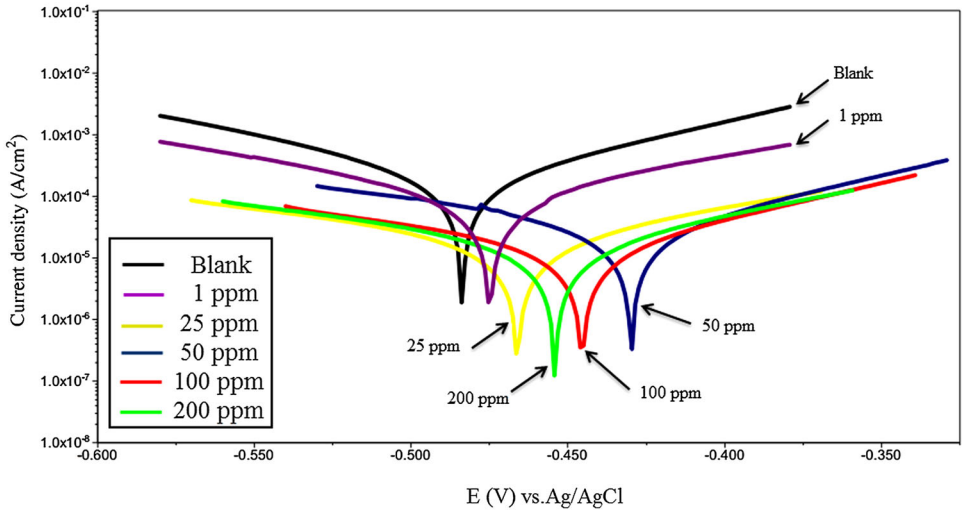

Fig. 6 Potentiodynamic polarization curves of low carbon steel in 1 M HCl in the absence and presence of different concentrations of CS at 25 °C (Color figure online)

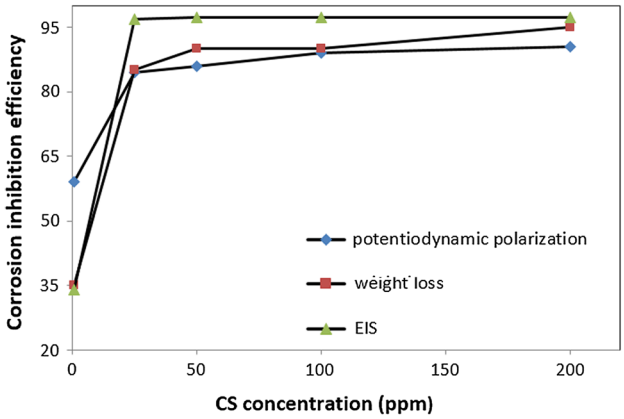

Fig. 7 The comparison of different IE measurements: IE_{wl} (%), IE_{EIS} (%), and IE_{Pol} (%) under different inhibitor concentrations

efficiency in acidic solution. The value of double-layer capacitance decreases from 86.2 (μF/cm^2) in blank to 19.1 (μF/cm^2) in presence of 25 ppm of the surfactant. Thus in system with higher R_t and lower C_{dl}, inhibition efficiency is more appropriate. Also, EIS measurements confirm the weight loss results.

Figure 6 represents potentiodynamic polarization curves of steel samples treated at different surfactant concentrations in 1 M HCl. As can be inferred, the inhibitor caused a significant reduction in the corrosion rate and the anodic curves shifted to more positive potentials and the cathodic curves altered to more negative potentials to lower values of current densities. Precisely, CS in 1 M HCl inhibits both cathodic hydrogen evolution and anodic Fe dissolution reactions of low carbon steel electrode corrosion. Adsorption of inhibitor over the corroded surface may be the reason for the observed behavior. Corrosion current densities (i_{corr}), corrosion potential (E_{corr}) and the inhibition efficiency (IE_{pol}) for different samples, were derived from the polarization curves and are listed in Table 3. According to the given data in Table 3, a sharp reduction in corrosion current density is seen. IE_{pol} increases with the inhibitor concentration which indicates that the presence of CS retards the dissolution of low carbon steel in 1 M HCl and the degree of inhibition depends on the concentration. For example, the IE_{pol} calculated from i_{corr} for the 25 ppm CS reaches a considerable value of 84.5%. From Fig. 6 it is clear that both the anodic and cathodic Tafel slopes slightly change upon addition of CS, which indicates that the inhibitor affects both anodic and cathodic reactions and this surfactant is mixed-type inhibitor (Ref 11, 18, 27, 33). In addition, from Table 3 it is clear that the values of E_{corr} did not change significantly, indicating that this substance acts as mixed-type corrosion inhibitor and a compound is usually classified as an anodic or cathodic type inhibitor.

On the basis of published data, the corrosion inhibition efficiency of an inhibitor can be obtained using different methods. One can be deduced from Fig. 7 is that an increase in inhibitor concentration resulted in an increase of the inhibition effects of the inhibitor on the corrosion of low carbon steel in HCl solution. The same results were obtained using weight loss, electrochemical impedance, and potentiodynamic polarization. It can be clearly seen that corrosion inhibition values obtained from EIS measurements are higher than those obtained from potentiodynamic polarization and weight loss measurements. The main reason contributing to the higher corrosion inhibition efficiency value obtained from EIS in comparison with potentiodynamic polarization and weight loss could be linked to the higher experimental duration for the impedance study (Ref 34). The experimental duration for the impedance study (which was about 15 min) was higher than polarization and weight loss measurements which were about 3.33 and 0 min. It is noteworthy that immersion times of all of the samples before corrosion immersion were about 60 min.

3.2 Effect of Immersion Time

The effect of immersion time on the corrosion rate of the steel in the presence of surfactant was investigated with weight loss method. Steel samples were immersed in 25 ppm of surfactant and 1 M HCl for 1-24 h (Fig. 8). The inhibition efficiency (IE_{wl} %) increased from 86 to 91% as the growth in time of immersion (1-3 h). From 91 to 85% reduction of

inhibition efficiency is seen when immersion time increased to 12 h (3-12 h). It is clear from Fig. 8 that for up to 3 h of immersion, multi-layer of inhibitor molecules is settled on the surface of steel and this may be a reason for achieving more inhibition efficiency. The hydrocarbon chains of some adsorbed cations are believed to leave the surface and aggregate to form hemi-micelle (Ref 7). The hemi-micelle phase in the surfactant solution means the start point to collect the surfactant in duplet, triplet, or quadrate before forming the complete micelles. This will cause the decrease of the effective area covered by surfactant molecules to some extent during 3-12 h. At higher immersion time (12-18 h), aggregation of micelles on the surface acts like an inhibitive layer.

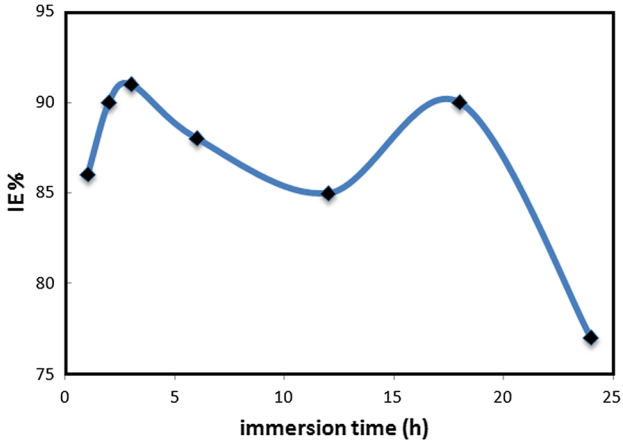

Fig. 8 Inhibition efficiency vs. immersion time of low carbon steel in 1 M HCl in the presence of 25 ppm surfactant at 25 °C

Table 4 Data obtained from potentiodynamic polarization tests for low carbon steel in 1 M HCl in the absence and presence of 25 ppm CS at various temperatures

T (°C)	Surfactant	i_{corr} (μA/cm^2)	E_{corr} (V vs. Ag/AgCl)	IE%
25	Blank	200	−0.484	…
	25 ppm	32.87	−0.466	84.5
30	Blank	139	−0.428	…
	25 ppm	48.9	−0.436	67
40	Blank	64	−0.425	…
	25 ppm	43.3	−0.416	33
50	Blank	23.5	−0.416	…
	25 ppm	103.5	−0.425	Corrosive

3.3 Effect of Temperature

The mode of inhibitor adsorption on the metal surface in those corrosion studies which involve the use of inhibitors substantially relies on the temperature variation. Hence the significance of temperature variation is to determine the mode of inhibitor adsorption (Ref 35). The effect of temperature on the corrosion behavior of low carbon steel was studied by EIS and

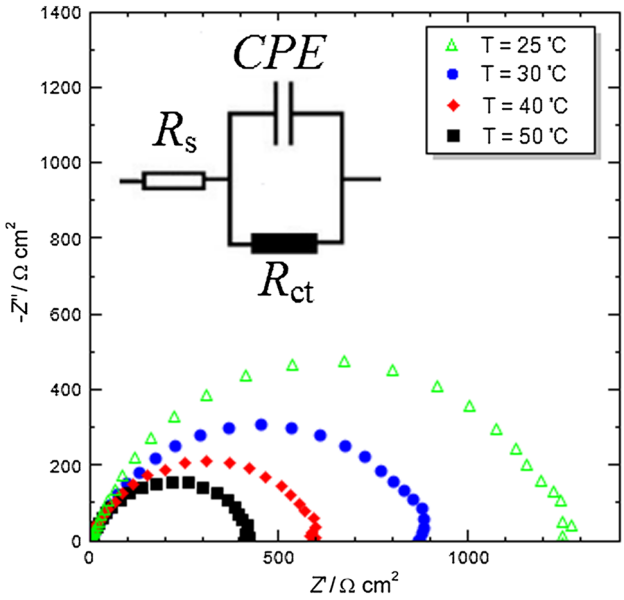

Fig. 10 Nyquist plots for low carbon steel in 1 M HCl in the absence and presence of 25 ppm CS at various temperatures in the range 25-30-40-50 °C

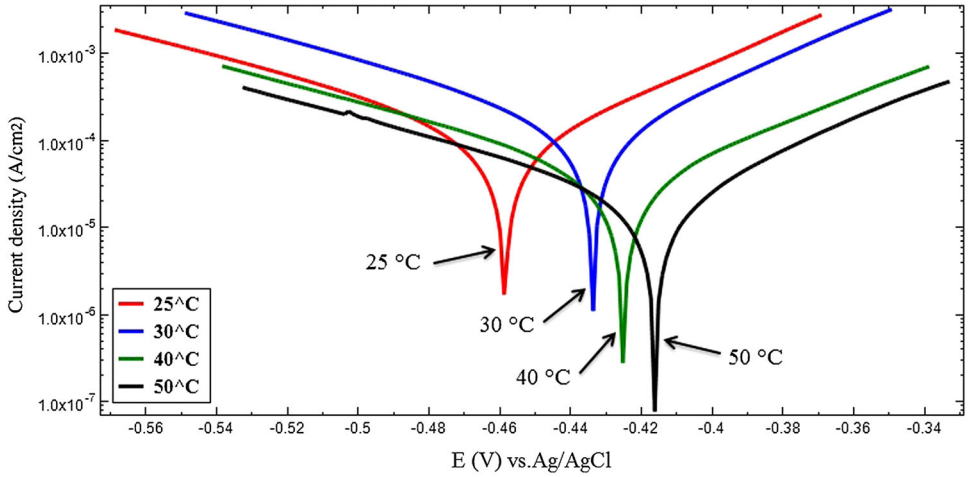

Fig. 9 Polarization curves of low carbon steel in 1 M HCl in the absence and presence of 25 ppm CS at various temperatures in the range (a) 25 °C, (b) 30 °C, (c) 40 °C, and (d) 50 °C (Color figure online)

potentiodynamic polarization methods at various temperatures at the value of 25-30-40-50 °C in the absence and presence of 25 ppm CS in 1 M HCl media. All experiments were carried out in solutions at a fixed temperature (25-30-40-50 °C).

Electrochemical parameters obtained by Tafel extrapolation method at different temperatures are given in Table 4. Anodic and cathodic polarization curves at various temperatures are shown in Fig. 9. The anodic and cathodic current densities increase with increasing temperature in inhibited solutions, with a slight positive shift in the corrosion potential values. The corrosion current density of low carbon steel decreases more rapidly with temperature in the absence of inhibitors. This is due to the formation of oxide layers as a result of corrosion reactions and consequently results in decrease of the corrosion current density.

It can also be seen from Table 4 that the inhibition efficiency values of CS decline as the temperature increase. So, continuous decrease of the parameter with temperature might indicate the progression of corrosion process on the metallic surface. Moreover, the behavior could lead one to believe that formation of the CS layer on the surface at high temperature occurs mainly through physical absorption. Hence, solution temperature is influential on the effectiveness of the surfactant. This phenomenon has been explained in some published studies that the desorption of the inhibitor molecules at higher temperature from the surface of alloy causes more area of metal which is exposed to aggressive solution (Ref 19, 31, 36). At 25 °C the highest level of protection was obtained in the presence of CS. Corrosion current density (i_{corr}) increases with increasing the temperature from 25 to 50 °C from 32 to 103 μA, respectively, and polarization resistance decreases. When the solution temperature is equal to 50 °C, the addition of CS has a negative effect on the corrosion protection properties.

Table 5 Obtained data from electrochemical impedance measurements of low carbon steel in 1 M HCl in the absence and presence of 25 ppm CS at various temperatures

T (°C)	Surfactant	R_s (Ω cm^2)	R_{ct} (Ω cm^2)	N	Y_0	C_{dl} (μF/cm^2)	IE%
25	Blank	17.7	52.2	0.9	154	84.9	…
	25 ppm	2.48	1310	0.77	854	19.1	96
30	Blank	1.91	82.6	0.91	191	108	…
	25 ppm	2.61	894	0.76	100	25.6	91
40	Blank	1.48	230.6	0.82	137	34.5	…
	25 ppm	1.03	741	0.76	124	18.6	68
50	Blank	1.69	384	0.82	44.9	11.7	…
	25 ppm	3.69	440	0.76	98.3	22.6	34

For better understanding the role of temperature on the efficiency of CS, the Nyquist plots of low carbon steel in the presence 25 ppm of CS at various temperatures are depicted in Fig. 10. The values of charge transfer resistance R_{ct}, double-layer capacitance C_{dl} and IE obtained after simulating with equivalent circuit are given in Table 5. According to Fig. 10 and Table 5, with increasing temperature, the value of charge transfer resistance decreases from 1310 (25) to 440 Ω cm^2 (50 °C) and consequently inhibition efficiency declines from 96 to 34%. Based on the results, both polarization and EIS are in good agreement with each other and it can be seen that EIS measurements confirm the polarization results and the value of inhibition efficiency of CS decreases with increase in solution temperature.

3.4 Effect of Addition of $NaHSO_4$

Corrosion rates of low carbon steel in 1 M HCl in the presence of cationic surfactant of 25 ppm and $NaHSO_4$ in different concentrations (0.001-0.1 M) were determined. The inhibition efficiency was calculated, and plots of potentiodynamic polarization curves and Nyquist diagrams are shown in Fig. 11 and 12 respectively. It was found that the inhibition efficiency for steel in 1 M HCl by the cationic surfactant in 25 ppm was 84.5%. On the other hand, the addition of $NaHSO_4$ in the above system resulted in a sharp increase in inhibition efficiency. Also, increase in $NaHSO_4$ concentration leads to more inhibition efficiency.

The synergistic effect between cationic surfactant and hydrogen sulfate ion for the corrosion inhibition of steel in 1 M HCl is investigated in Tables 6 and 7. Inhibition efficiency increases from 84.5% in presence of 25 ppm surfactant without any salt, up to 99%, in presence of 25 ppm surfactant and 0.1 M of $NaHSO_4$ (from potentiodynamic polarization

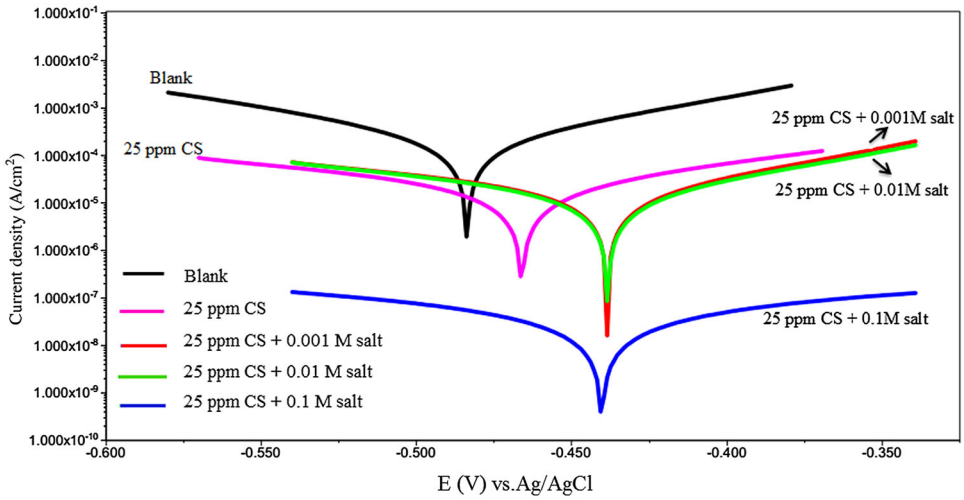

Fig. 11 Potentiodynamic polarization curves of low carbon steel in 1 M HCl with the presence CS + different concentrations of $NaHSO_4$ salt (Color figure online)

experiment). Co-adsorption of molecules which is either competitive or co-operative can be the rationale for the synergistic effect of halide ions with surfactant molecules (Ref 33, 37). The anion and cation are adsorbed at different sites on the metal where the adsorption is competitive. In co-operative adsorption, cation was absorbed on a layer of anion, which absorbed chemically previously (Ref 38). In the presence of a salt, the surfactant cation is expected to make a complex structure as a result of strong chemisorption with HSO_4^- ions of salts, which could facilitate the adsorption of ionic liquid cations on the positively charged surface of the metal. Inhibitors are adsorbed on the metal surface by coloumbic attraction where the HSO_4^- ions were adsorbed by chemisorption previously.

Higher surface coverage results from stabilization of adsorbed HSO_4^- ions with cationic form inhibitor so that more inhibition is achieved (Ref 24).

3.5 AFM Study

The AFM provides a powerful means of characterizing microstructure, and was implemented to show the impact which inhibitors make on the metal/solution interface (Ref 1, 2). The two (2D) and three-dimensional (3D) AFM images and height profiles of low carbon steel surface before immersion are shown in Fig. 13(a). According to Fig. 13(a), prior to immersion, the surface of steel is smooth and has some sign of

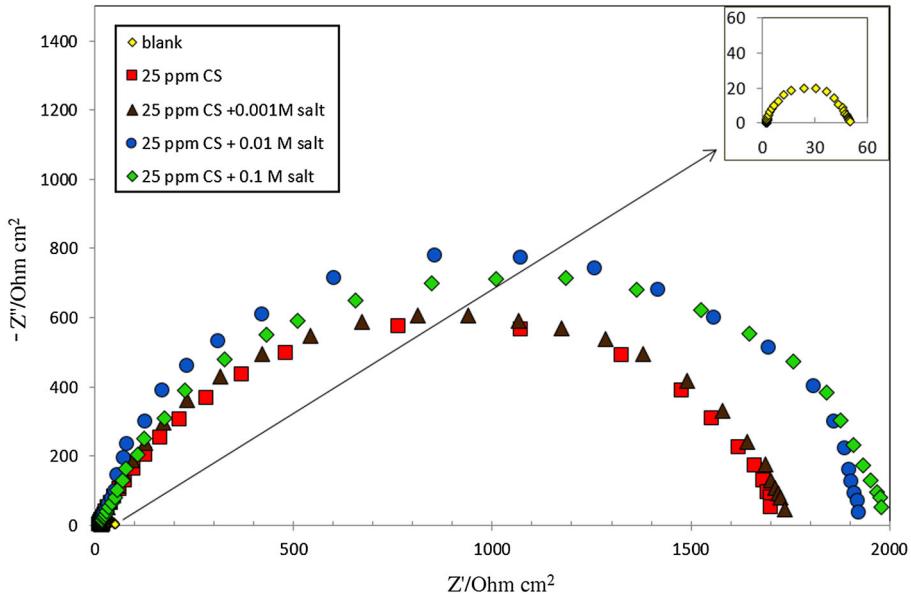

Fig. 12 Nyquist plots of low carbon steel in 1 M HCl without and with CS + different concentrations of $NaHSO_4$ salt

Table 6 Data obtained fr$_4$om potentiodynamic polarization of low carbon steel in 1 M HCl without and with CS + different concentrations of NaHSO salt calculated by the Tafel extrapolation method

1 M HCl + *x* ppm surfactant	i_{corr} (μA/cm^2)	E_{corr} (V vs. Ag/AgCl)	IE%
Blank	200	−0.484	…
25 ppm CS	31	−0.466	84.5
25 ppm CS + 0.001 M salt	20	−0.438	90
25 ppm CS + 0.01 M salt	19.4	−0.439	90.3
25 ppm CS + 0.1 M salt	1	−0.44	99

Table 7 Data obtained from EIS of low carbon steel in 1 M HCl without and with CS + different concentrations of $NaHSO_4$ salt

System inhibitor	R_s (Ω)	R_{ct} (Ω)	N	Y_0	C_{dl} (μF cm^2)	IE%
Blank	17.7	52.2	0.9	154	84.9	…
25 ppm surfactant	2.7	1668	0.78	85.5	19.1	96.8
25 ppm surfactant + 0.001 M $NaHSO_4$	2.58	1740	0.8	94.2	23.3	96.9
25 ppm surfactant + 0.01 M $NaHSO_4$	3.96	1910	0.85	58.3	21.9	97.2
25 ppm surfactant + 0.1 M $NaHSO_4$	2.34	1970	0.78	78.3	28.6	97.3

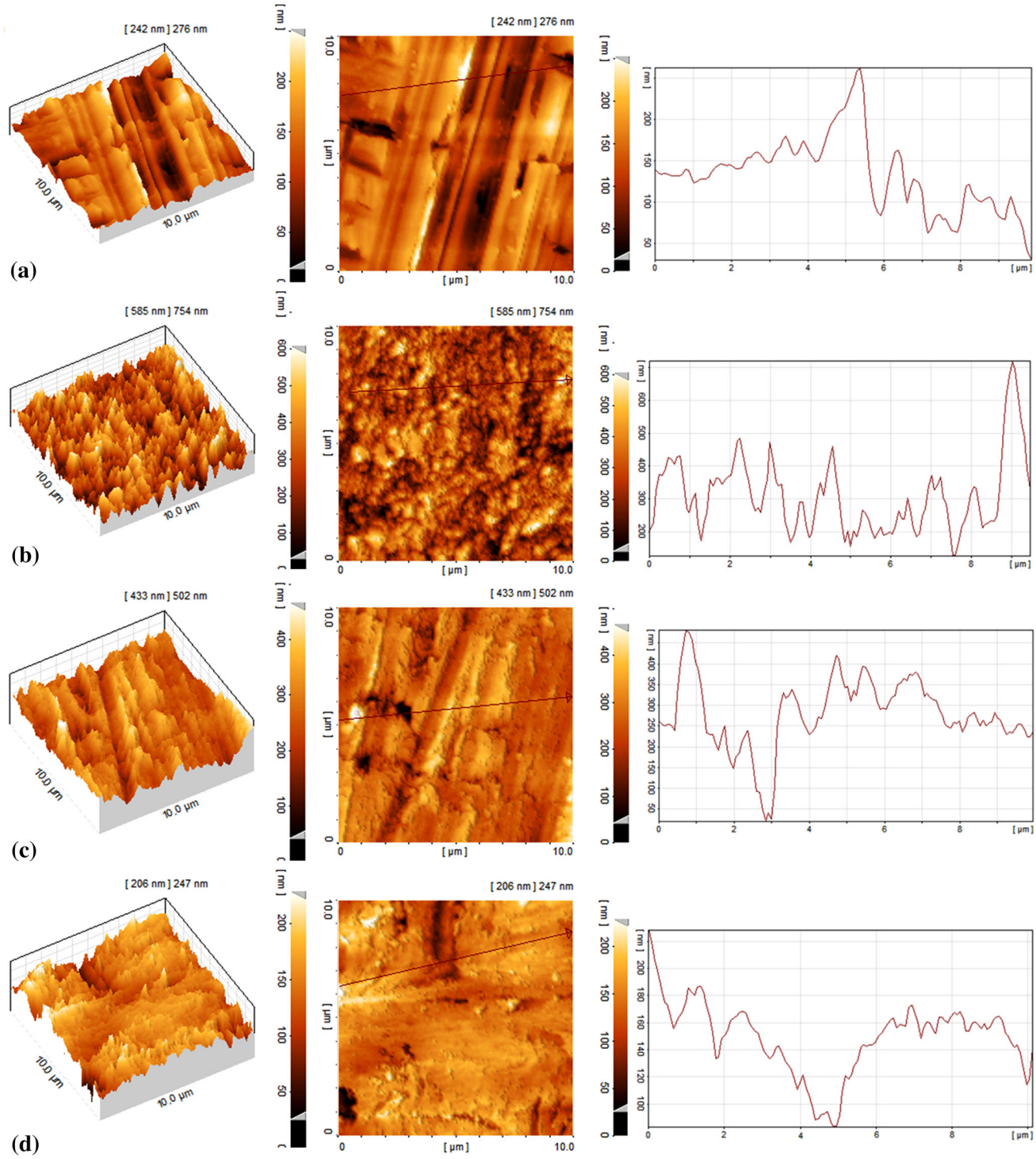

Fig. 13 AFM micrograph of the low carbon steel before immersion in 1 M HCl (a) after 1 h of immersion in 1 M HCl (b) 25 ppm CS + 1 M HCl (c) 25 ppm CS + 0.1 M $NaHSO_4$ + 1 M HCl (d)

abrading but it still has some crevices that are covered with 'granule,' which may be attributed to the defects in steel, and probably an oxide inclusion (Ref 3, 18). On the basis of Fig. 13(b), the steel surface after immersion in uninhibited 1 M HCl for 1 h was damaged strongly in comparison with Fig. 13(a), and covered with corrosion products. Establishing a comparison between Fig. 13(c) and (b) clarifies the existence of an adsorptive film in the presence of 25 ppm CS. Therefore, it might be deduced that these particles are related to adsorption film of the inhibitor, which inhibits the corrosion of steel (Ref 4, 5). After modification with $NaHSO_4$, the surface morphology was changed to a compact and uniform film (Fig. 13d).

Micrograph of steel surface before immersion shows small particles on the surface and the surface roughness of the steel is 32.8 nm from Fig. 13(a). Figure 13(b) indicates that after immersion of the substrate into 1 M HCl solution, the surface roughness showed an increase to 602 nm, while immersion in a

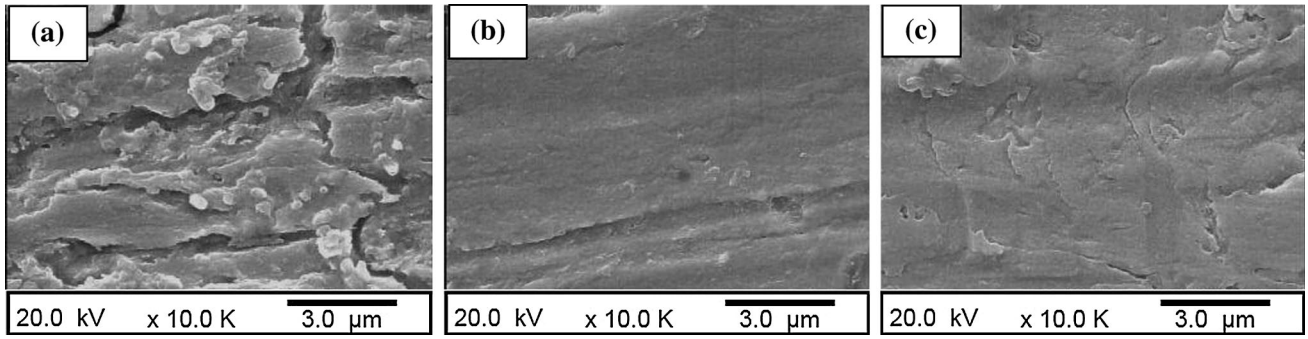

Fig. 14 The SEM images for the low carbon steel surface after immersion for 1 h in 1 M HCl (a), with 25 ppm of CS (b), and with 25 ppm of CS + 0.1 M $NaHSO_4$ (c)

solution containing reduced the roughness to 117 nm (Fig. 13c).

3.6 FE-SEM Study

The morphologies of low carbon steel surface immersed in the corrosion solution for 1 h in the absence and presence of various concentrations of surfactant at 25 °C are displayed in Fig. 14(a)-(c). The micrograph reveals that the surface was strongly damaged in the absence of the surfactant (Fig. 14a). This is concluded from the large pits and fracture visible, while the low carbon steel surface exposed to various concentrations of surfactant was smooth (Fig. 14b and c). Obviously, the surface is free of any corrosion products. According to Fig. 14(b), the surface of the sample has the same level of smoothness as the polished surface, although the polished surface has trace of scratches. For 25 ppm concentration of CS, the micrograph shown in Fig. 14(b) does not show a protective film on the surface. However, as the EIS and potentiodynamic polarization test results stated, there should be a protective film on the surface. Most probably the protective film is not recognizable by SEM technique. For combination of CS and $NaHSO_4$, the micrograph (Fig. 14c) depicts that a uniform and compact protective film settled on the steel surface. This could be due to involvement of the cationic surfactant molecules with the reaction sites of iron surface, which decreases the contact between iron and the aggressive media (Ref 11).

4. Conclusions

The results can be summarized as follows:

1. According to the results with the use of cationic surfactant, 1-methyl-3-octadecane imidazolium hydrogen sulfate, a dramatic improvement in corrosion inhibition for low carbon steel in 1 M HCl solution is observed.
2. It was found that more the concentration of the surfactant, the more percentage inhibition efficiency is gained.
3. The corrosion inhibition of low carbon steel is because of the adsorption of the inhibitor molecules on low carbon steel surface and blocking of its active sites.
4. The EIS measurements are an indication of the fact that the charge transfer resistance (R_{ct}) increases with increasing concentration of inhibitor, while the double-layer capacitance is decreased.
5. The corrosion current density (i_{corr}) diminishes with the growth of the concentration of surfactant, which implies that the presence of CS retards the dissolution of low carbon steel in 1 M HCl and the degree of inhibition is dependent upon the concentration and based on the polarization results; the investigated surfactant acted as mixed inhibitor.
6. Addition of CS into 1 M HCl solution facilitates the formation of a fully uniform film on the steel surface, which resulted in the reduction of the steel surface roughness and increasing protective performance of steel from corrosion.
7. DC and AC measurements are in agreement with the fact that a rise in temperature lessens the inhibition efficiency.
8. A synergetic effect derived from $NaHSO_4$ in the presence of novel cationic surfactant has been confirmed by electrochemical and FE-SEM studies.

References

1. F. Zucchi, G. Trabanelli, and G. Brunoro, The Influence of the Chromium Content on the Inhibitive Efficiency of Some Organic Compounds, *Corros. Sci.*, 1992, **33**(7), p 1135–1139
2. M. Elachouri, M.S. Hajji, S. Kertit, E.M. Essassi, M. Salem, and R. Coudert, Some Surfactants in the Series of 2-(Alkyldimethylammonio) Alkanol Bromides as Inhibitors of the Corrosion of Iron in Acid Chloride Solution, *Corros. Sci.*, 1995, **37**(3), p 381–389
3. I. Jevremovic, M. Singer, S. Nesic, and V. Miskovic, Stankovic, Inhibition Properties of Self-assembled Corrosion Inhibitor Talloil Diethylenetriamine Imidazoline for Mild Steel Corrosion in Chloride Solution Saturated with Carbon Dioxide, *Corros. Sci.*, 2013, **77**, p 265–272
4. X.H. Li, S.D. Deng, H. Fu, G.N. Mu, and N. Zhao, Synergism Between Rare Earth Cerium(IV) Ion and Vanillin on the Corrosion of Steel in H_2SO_4 Solution: Weight Loss, Electrochemical, UV-VIS, FTIR, XPS, and AFM Approaches, *Appl. Surf. Sci.*, 2008, **254**(17), p 5574–5586
5. X.H. Li, S.D. Deng, G.N. Mu, H. Fu, and F.Z. Yang, Inhibition Effect of Nonionic Surfactant on the Corrosion of Cold Rolled Steel in Hydrochloric Acid, *Corros. Sci.*, 2008, **50**(2), p 420–430
6. S. Bilgic and N. Caliskan, The Effect of N-(1-Toluidine) Salicylaldimine on the Corrosion of Austenitic Chromium–Nickel Steel, *Appl. Surf. Sci.*, 1999, **152**(1–2), p 107–114
7. M.A. Malik, M.A. Hashim, F. Nabi, S.A. Al-Thabaiti, and K. Khan, Review Anti-corrosion Ability of Surfactants: A Review, *Int. J. Chem. Sci.*, 2011, **6**(6), p 1927–1948
8. L.G. Qiu, A.J. Xie, and Y.H. Shen, A Novel Triazole-Based Cationic Gemini Surfactant: Synthesis and Effect on Corrosion Inhibition of Carbon Steel in Hydrochloric Acid, *Mater. Chem. Phys.*, 2005, **91**(2–3), p 269–273
9. M. Mobin and S. Masroor, Adsorption and Corrosion Inhibition Behavior of Schiff Base-Based Cationic Gemini Surfactant on Mild

Steel in Formic Acid, *J. Dispersion Sci. Technol.*, 2014, **35**(4), p 535–543
10. A.A. El Maghraby and T.Y. Soror, Efficient Cationic Surfactant as Corrosion Inhibitor for Carbon Steel in Hydrochloric Acid Solutions, *Adv. Appl. Sci. Res.*, 2010, **1**(2), p 156–168
11. M. Motamedi, A.R. Tehrani-Bagha, and M. Mahdavian, Effect of Aging Time on Corrosion Inhibition of Cationic Surfactant on Mild Steel in Sulfamic Acid Cleaning Solution, *Corros. Sci.*, 2013, **70**, p 46–54
12. V.M. Abbasov, H.M. Abd El-Lateef, L.I. Aliyeva, E.E. Qasimov, I.T. Ismayilov, A.H. Tantawy, and S.A. Mamedxanova, Applicability of Novel Anionic Surfactant as a Corrosion Inhibitor of Mild Steel and for Removing Thin Petroleum Films from Water Surface, *Am. J. Mater. Sci. Eng.*, 2013, **1**(2), p 18–23
13. J.R. Kanicky, J.C. Lopez-Montilla, S. Pandey, and D.O. Shah, Surface Chemistry in the Petroleum Industry, *Handbook of Applied Surface and Colloid Chemistry*, K. Holmberg, Ed., Wiley, Gainesville, FL, 2001, p 251–267
14. M.J. Rosen, Adsorption of Surface-Active Agents at Interfaces: The Electrical Double Layer, *Surfactants and Interfacial Phenomena*, M.J. Rosen, Ed., Wiley, Hoboken, NJ, 2004, p 34–73
15. E. Kowsari and I. Yavari, *Green Chemistry-A New Paradigm of Organic Synthesis Using ILs*, LAP Academic Publishing, New York, 2011
16. L.G. Qiu, A.J. Xie, and Y.H. Shen, Understanding the Adsorption of Cationic Gemini Surfactants on Steel Surface in Hydrochloric Acid, *Mater. Chem. Phys.*, 2004, **87**(2–3), p 237–240
17. D. Asefi, M. Arami, and N.M. Mahmoodi, Electrochemical Effect of Cationic Gemini Surfactant and Halide Salts on Corrosion Inhibition of Low Carbon Steel in Acid Medium, *Corros. Sci.*, 2010, **52**(3), p 794–800
18. D. Asefi, M. Arami, and N.M. Mahmoodi, Effect of Nonionic Co-surfactants on Corrosion Inhibition Effect of Cationic Gemini Surfactant, *Colloids Surf. A*, 2010, **355**(1–3), p 183–186
19. M.A. Hegazy, A Novel Schiff Base-Based Cationic Gemini Surfactants: Synthesis and Effect on Corrosion Inhibition of Carbon Steel in Hydrochloric Acid Solution, *Corros. Sci.*, 2009, **51**(11), p 2610–2618
20. X. Li, S. Deng, H. Fu, and G. Mu, Inhibition Effect of 6-Benzylaminopurine on the Corrosion of Cold Rolled Steel in H_2SO_4 Solution, *Corros. Sci.*, 2009, **51**(3), p 620–634
21. H. Otmacic and E. Stupnisek-Lisac, Copper Corrosion Inhibitors in Near Neutral Media, *Electrochim. Acta*, 2003, **48**(8), p 985–991
22. M.A. Migahed, Electrochemical Investigation of the Corrosion Behaviour of Mild Steel in 2 M HCl Solution in Presence of 1-Dodecyl-4-Methoxy Pyridinium Bromide, *Mater. Chem. Phys.*, 2005, **93**(1), p 48–53
23. R. Fuchs-Godec, Effects of Surfactants and Their Mixtures on Inhibition of the Corrosion Process of Ferritic Stainless Steel, *Electrochim. Acta*, 2009, **54**(8), p 2171–2179
24. L.E. Zerpa, J.L. Salager, C.A. Koh, E. Dendy, and A.K. Sum, Surface Chemistry and Gas Hydrates in Flow Assurance, *Ind. Eng. Chem. Res.*, 2011, **50**(1), p 188–197
25. M.E. Achouri, N.M. Infante, F. Izquierdo, S. Kertit, H.M. Gouttaya, and B. Nciri, Synthesis of Some Cationic Gemini Surfactants and Their Inhibitive Effect on Iron Corrosion in Hydrochloric Acid Medium, *Corros. Sci.*, 2001, **43**(1), p 19–35
26. D. Asefi, M. Arami, A.A. Sarabi, and N.M. Mahmoodi, The Chain Length Influence of Cationic Surfactant and Role of Nonionic Co-surfactants on Controlling the Corrosion Rate of Steel in Acidic Media, *Corros. Sci.*, 2009, **51**(8), p 1817–1821
27. F.M. Menger and J.S. Keiper, Gemini Surfactants, *Angew. Chem. Int. Ed.*, 2000, **39**, p 1906–1920
28. H. Ma, S. Chen, B. Yin, S. Zhao, and X. Liu, Impedance Spectroscopic Study of Corrosion Inhibition of Copper by Surfactants in the Acidic Solutions, *Corros. Sci.*, 2003, **45**(5), p 867–882
29. M.A. Hegazy and M.F. Zaky, Inhibition Effect of Novel Nonionic Surfactants on the Corrosion of Carbon Steel in Acidic Medium, *Corros. Sci.*, 2010, **52**(4), p 1333–1341
30. V. Branzoi, F. Branzoi, and M. Baibarac, The Inhibition of the Corrosion of Armco Iron in HCl Solutions in the Presence of Surfactants of the Type of N-Alkyl Quaternary Ammonium Salts, *Mater. Chem. Phys.*, 2000, **65**(3), p 288–297
31. F.A. Ansari and M.A. Quraishi, Inhibitive Performance of Gemini Surfactants as Corrosion Inhibitors for Mild Steel in Formic Acid, *Portugaliae Electrochim. Acta*, 2010, **28**(5), p 321–335
32. H. Eivaz Mohammadloo, A.A. Sarabi, A.A. Sabbagh Alvani, H. Sameie, and R. Salimi, Nano-ceramic Hexafluorozirconic Acid Based Conversion Thin Film: Surface Characterization and Electrochemical Study, *Surf. Coat. Technol.*, 2012, **206**(19–20), p 4132–4139
33. M.A. Deyab, Effect of Cationic Surfactant and Inorganic Anions on the Electrochemical Behavior of Carbon Steel in Formation Water, *Corros. Sci.*, 2007, **49**(5), p 2315–2328
34. S.Y. Arman, R. Naderi, and B. PouryosefiMarkhalia, Effect of DC Trend Removal and Window Functioning Methods on Correlation Between Electrochemical Noise Parameters and EIS Data of Stainless Steel in an Inhibited Acidic Solution, *RSC Adv.*, 2014, **4**(73), p 39045–39057
35. X. Wang, H. Yang, and F. Wnag, A Cationic Gemini-Surfactant as Effective Inhibitor for Mild Steel in HCl Solutions, *Corros. Sci.*, 2010, **52**(4), p 1268–1276
36. X. Li, L. Tang, H. Liu, G. Mu, and G. Liu, Influence of Halide Ions on Inhibitive Performance of Cetyl Trimethyl Ammonium Bromide in Various Concentrations of Phosphoric Acid for Cold Rolled Steel, *Mater. Lett.*, 2008, **62**(15), p 2321–2324
37. I.B. Obot, N.O. Obi-Egbedi, and S.A. Umoren, The Synergistic Inhibitive Effect and Some Quantum Chemical Parameters of 2,3-Diaminonaphthalene and Iodide Ions on the Hydrochloric Acid Corrosion of Aluminium, *Corros. Sci.*, 2009, **51**(2), p 276–282
38. A. Fiala, A. Chibani, A. Darchen, A. Boulkamh, and K. Djebbar, Investigations of the Inhibition of Copper Corrosion in Nitric Acid Solutions by Ketene Dithioacetal Derivatives, *Appl. Surf. Sci.*, 2007, **253**(24), p 9347–9356